Biochemistry

 Volume 39, Number 9 March 7, 2000

Accelerated Publications

Simultaneous Binding of Two DNA Duplexes to the NtrC−Enhancer Complex Studied by Two-Color Fluorescence Cross-Correlation Spectroscopy†

Karsten Rippe*

Deutsches Krebsforschungszentrum, Abteilung Biophysik der Makromoleküle, Im Neuenheimer Feld 280, D-69120 Heidelberg, Germany

Received September 23, 1999; Revised Manuscript Received December 16, 1999

ABSTRACT: The transcription activator protein NtrC (nitrogen regulatory protein C, also termed NR_I) can catalyze the transition of *Escherichia coli* RNA polymerase complexed with the σ^{54} factor (RNAP·σ^{54}) from the closed complex (RNAP·σ^{54} bound at the promoter) to the open complex (melting of the promoter DNA). This process involves phosphorylation of NtrC (NtrC-P), assembly of an octameric NtrC-P complex at the enhancer DNA sequence, interaction of this complex with promoter-bound RNAP·σ^{54} via DNA looping, and hydrolysis of ATP. Here it is demonstrated by two-color fluorescence cross-correlation spectroscopy measurements of 6-carboxyfluorescein and 6-carboxy-X-rhodamine-labeled DNA oligonucleotide duplexes that the NtrC-P complex can bind two DNA duplexes simultaneously. This suggests a model for the conformation of the looped intermediate that is formed between NtrC-P and RNAP·σ^{54} at the *glnA*p2 promoter during the activation process.

The enhancer-binding factor NtrC[1] from enteric bacteria is a transcription activator protein of RNAP·σ^{54} (*1*, *2*). It regulates a variety of genes that are involved in nitrogen utilization. The location of the NtrC binding sites found in vivo requires looping of the DNA for interaction with RNAP·σ^{54} at the *glnA*p2 promoter (*3*−*7*). NtrC activity is regulated by phosphorylation of the protein at Asp54 of the conserved receiver domain (*1*, *2*). In vivo, the histidine kinase NtrB (nitrogen regulatory protein B) autophosphorylates under nitrogen limitation conditions and serves as a phosphate donor for the phosphorylation of NtrC. This reaction can be reproduced in vitro in the absence of NtrB by the addition of a phosphorylating chemical-like carbamyl phosphate (*8*). NtrC is a dimer in solution (*9*, *10*) and binds as a dimer to a single binding site as shown by gel electrophoretic analysis (*11*) and analytical ultracentrifugation (*10*). In the latter study, it was also demonstrated that phosphorylated NtrC (NtrC-P) forms an octameric complex in the presence of an oligonucleotide duplex with two binding sites. Results from scanning force microscopy and gel filtration analysis of NtrC and various mutants in conjunction with in vitro transcription experiments are consistent with the formation of a NtrC-P octamer at the enhancer but can also be explained by a hexameric NtrC-P complex as discussed in ref *12*. Various lines of evidence indicate that the oligomerization of phosphorylated NtrC dimers is required for the formation of an active NtrC complex (*1*, *2*, *11*−*15*).

In the study presented here, it was examined whether the NtrC-P complex is able to bind two DNA strands simultaneously. To address this question, a new approach has been

† This work was supported by DFG Grant Ri 828/1.

* Corresponding author. Telephone: +49-6221-423392. Fax: +49-6221-423391. E-mail: Karsten.Rippe@dkfz-heidelberg.de.

[1] Abbreviations: FCS, fluorescence correlation spectroscopy; FCCS, two-color fluorescence cross-correlation spectroscopy; NtrC, nitrogen regulatory protein C; NtrC-P, phosphorylated NtrC; RNAP, RNA polymerase; FAM, 6-carboxyfluorescein; ROX, 6-carboxy-X-rhodamine.

10.1021/bi9922190 CCC: $19.00
Published on Web 02/29/2000

used that is based on fluorescence correlation spectroscopy (FCS) (reviewed in refs *16* and *17*). FCS measures mean diffusion times and concentrations by evaluating fluctuations of the fluorescence intensity that have their origin in the Brownian motion of fluorophores through a small volume element. This volume element of about 1 fL is defined by the focus of the excitation light beam. The measured fluctuations of the fluorescence signal depend on the speed at which the fluorophores move through the focus and are therefore related to the diffusion coefficient. If the intensity fluctuations of two different dyes are evaluated in separate channels, a fluorescence cross-correlation (FCCS) signal between the two dyes can be obtained (*16*, *18*−*23*). With FCCS, a detection and selective analysis of molecules that carry both fluorophores is possible. In these experiments, the normalized cross-correlation function $G_x(\tau)$ is recorded which is calculated as the time average $\langle\ \rangle$ of the fluctuations of the detected fluorescence $\delta F_f(t)$ of one dye at time t and the fluctuations $\delta F_r(t + \tau)$ of the second dye at the delayed time $t + \tau$ (*16*, *18*−*20*).

$$G_x(\tau) = \frac{\langle \delta F_f(t)\, \delta F_r(t+\tau)\rangle}{\langle F_f(t)\rangle \langle F_r(t)\rangle} \quad (1)$$

Indices f and r denote the two detection channels that are correlated with each other. For the cross-correlation function $G_x(\tau)$, one fluorophore is measured in channel f (here 6-carboxyfluorescein abbreviated as FAM or fluorescein) and the other in channel r (here 6-carboxy-X-rhodamine abbreviated as ROX or rhodamine). Only molecules that carry both labels contribute to the measured fluctuations of the fluorescence signal. When f is the same as r, that is for correlation of the signals from only one fluorophore in the appropriate detection channel, eq 1 becomes the autocorrelation function $G_0(\tau)$ given in eq 2 (*16*, *17*).

$$G_0(\tau) = \frac{\langle \delta F(t)\, \delta F(t+\tau)\rangle}{\langle F(t)\rangle^2} \quad (2)$$

For n noninteracting species, eq 2 results in eq 3 (*22*, *24*):

$$G_0(\tau) = \frac{\sum_{i=1}^{n} \langle F_i(t)\rangle^2 G_{0,i}(\tau)}{\left[\sum_{i=1}^{n} \langle F_i(t)\rangle\right]^2} \quad (3)$$

At $\tau = 0$, the values of the autocorrelation function $G_0(0)$ and the cross-correlation function $G_x(0)$ are obtained.

$$G_0(0) = \frac{\langle \delta F(t)^2\rangle}{\langle F(t)\rangle^2} \quad (4)$$

$$G_x(0) = \frac{\langle \delta F_f(t)\, \delta F_r(t)\rangle}{\langle F_f(t)\rangle \langle F_r(t)\rangle} \quad (5)$$

These two quantities can be determined directly from the measured correlation curves even if multiple species are present. If only one species is present, the autocorrelation function $G_0(0)$ yields the average number of particles $\langle N\rangle$ in the focus volume (*17*).

$$G_0(0) = \frac{1}{\langle N\rangle} \quad (6)$$

As shown below, $G_0(0)$ and $G_x(0)$ reflect the average number of singly and doubly labeled molecules in the focus volume, respectively, and can be used for a quantitative detection of the simultaneous binding of ligands labeled with two different fluorophores.

MATERIALS AND METHODS

DNA and Protein Preparations. HPLC-purified DNA oligonucleotides covalently labeled via a hexyl linker at the 5′-end with 6-carboxyfluorescein (FAM) or 6-carboxy-X-rhodamine (ROX) were purchased from PE-Applied Biosystems (Weiterstadt, Germany). Purification of the three DNA duplexes ES-2_f, ES-2_r, and ES-2_{fr} (Figure 1) by gel electrophoresis was carried out according to ref *10*. The extinction coefficients of the single strands were determined as described previously (*25*). For the DNA duplexes, an ϵ_{260} of 876 000 M^{-1} cm^{-1} (ES-2_f), an ϵ_{260} of 884 000 M^{-1} cm^{-1} (ES-2_r), and an ϵ_{260} of 910 000 M^{-1} cm^{-1} (ES-2_{fr}) were derived, which are accurate within approximately 10%.

Expression and purification of His-tagged NtrC protein from plasmid pNTRC-3 were carried out according to ref *10*. The concentration of active NtrC dimers in the protein stock solution was determined from fluorescence anisotropy measurements by stoichiometric titrations to an oligonucleotide duplex with a single DNA binding site as described previously (*25*) to be 450 ± 70 nM. This value includes the 10% error in the determination of the DNA concentration. The binding reaction with the ES-2 DNA was conducted on ice for 2 h with a 200 μL solution of the indicated NtrC concentrations in a buffer containing 20 mM Tris-HCl (pH 7.9), 180 mM KCl, 10 mM $MgCl_2$, 20 mM carbamyl phosphate, 0.01% Nonidet P 40, 0.1 mM DTT, 0.1 mM EDTA, and 5% glycerol or in the same buffer in the absence of carbamyl phosphate. In the presence of carbamyl phosphate and $MgCl_2$, the NtrC protein is chemically phosphorylated so that a NtrC-P octamer complex forms with the ES-2 DNA duplex (*10*). For digestion of NtrC-P protein, 2 units of proteinase K (Roche Molecular Biochemicals, Mannheim, Germany) was added to a reaction mixture with preformed NtrC-P complexes with ES-2, and the sample was incubated for 1 h at 37 °C.

Instrumental Setup and Data Acquisition. FCS and FCCS measurements were conducted at 23 °C in triplicate with a new instrument developed in the laboratory of J. Langowski (*22*, *23*). An air-cooled argon/krypton ion laser (Laser 2000, Wessling, Germany) for excitation with linearly polarized light at 488 and 568 nm was focused by a water-immersion UPlanApo 60×/1.2W objective lens (Olympus Optical Co., Tokyo, Japan). The incident laser power inside the sample was set to about 2 μW at 488 nm, corresponding to an irradiance of ∼1.3 kW cm^{-2}. Detection was essentially unpolarized with count rates of about 6−7 kHz (fluorescein channel, 500−560 nm) and 60−70 kHz (rhodamine channel, 580−690 nm) for a dye concentration of 10 nM each, using a 50 μm pinhole in the confocal detection channel. The samples were measured in Lab-tek chamber slides with eight chambers and a ∼140 μm thick cover slide at the bottom (Nalge Nunc, Naperville, IL). The focus of the lens was

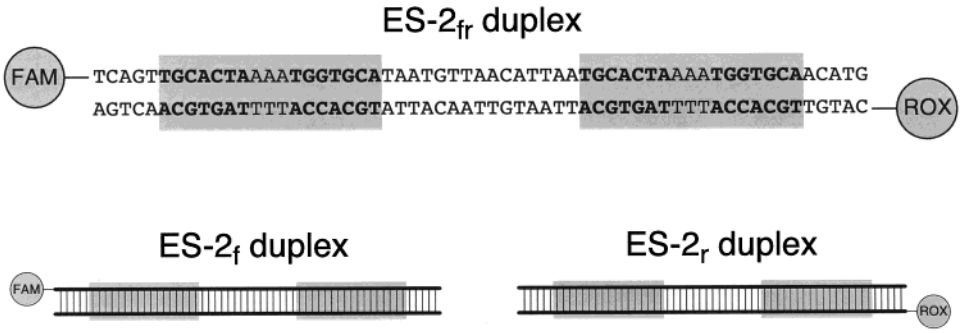

FIGURE 1: Oligonucleotide duplexes used in this study. The two NtrC binding sites are shaded gray, and the recognition sequence is printed in bold. ES-2 duplexes were labeled at the 5′-end with 6-carboxyfluorescein (FAM, ES-2_f duplex), 6-carboxy-X-rhodamine (ROX, ES-2_r duplex), or both dyes (ES-2_{fr} duplex). The doubly labeled duplex ES-2_{fr} was only used in the DNA experiments (Figure 2) but not in the experiments with NtrC and NtrC-P (Figure 3) which were conducted with a 1:1 mixture of ES-2_f and ES-2_r.

placed inside the solution to be analyzed and about 50 μm above the inner surface of the cover slide. Autocorrelation and cross-correlation functions were obtained by averaging 10 measurements of 30 s each. The sensitivity of the cross-correlation measurements was limited mostly by the ~10 times lower signal of FAM as compared to that of ROX. To improve the signal-to-noise ratio, DNA duplexes were also tested in which FAM was replaced with rhodamine green (data not shown). Although the free rhodamine green succinimidyl ester was about twice as bright as the corresponding FAM derivative, the intensity differences disappeared in the dye−DNA conjugates.

Data Analysis of FCS and FCCS Measurements. The values of the cross-correlation function $G_x(0)$ and the autocorrelation function of the rhodamine channel $G_{0,r}(0)$ at $\tau = 0$ were determined from a nonlinear least-squares fit to eq 7 for one, two, or three different species using the Levenberg−Marquardt algorithm implemented in the program *Quickfit* (*22*, *23*).

$$G(\tau) = 1 + \left[1 - \beta_T + \beta_T \exp\left(-\frac{\tau}{\tau_T}\right)\right]\frac{1}{\langle N\rangle}\sum_{i=1}^{n}\rho_i\left(1+\frac{\tau}{\tau_i}\right)^{-1}\left(1+\frac{\tau}{\tau_i\kappa^2}\right)^{-1/2} \quad (7)$$

Equation 7 describes the correlation function for n species with translational diffusion time τ_i present at the apparent fraction ρ_i. The structure factor κ is the axial ratio of the observation volume z_0/w_0. It was determined with a monodisperse solution of free rhodamine dye and was kept at a fixed value of 5 in the analysis of the data. For a given value of κ, the width of the detection volume w_0 is related to the diffusion coefficient D as shown in eq 8.

$$\tau = \frac{w_0^2}{4D} \quad (8)$$

The other two fit parameters in eq 7 are the triplet amplitude β_T and the triplet time constant τ_T. The contribution from the triplet state was only included for the fit of the autocorrelation functions but not for the cross-correlation function.

From the ratio $G_x(0)/G_{0,r}(0)$ (designated as ratio G), the fraction θ of DNA that was present in NtrC complexes with two DNA strands was calculated as described below. In the autocorrelation function of ROX, three different species are detected if two duplexes can bind. In terms of the average number of particles in the focus volume, these are the free ES-2 duplex with a single rhodamine label $\langle N_r\rangle$, a complex with one rhodamine and one fluorescein label $\langle N_{fr}\rangle$, and in the case of the experiments with NtrC-P also a protein complex with two rhodamine labels $\langle N_{rr}\rangle$. Molecules with one $\langle N_f\rangle$ or two fluorescein labels $\langle N_{ff}\rangle$ are not detected in the rhodamine channel except for some background contribution that is accounted for as described below. In the concentration range that was studied, the measured fluorescence intensity of a given dye-labeled species is proportional to the average number of molecules in the focus volume. Thus, for the rhodamine autocorrelation function at $\tau = 0$, eq 9 is derived from eq 3:

$$G_{0,r}(0) = \frac{q_{r,1}^2\langle N_r\rangle + q_{r,2}^2\langle N_{fr}\rangle + 4q_{r,3}^2\langle N_{rr}\rangle}{(q_{r,1}\langle N_r\rangle + q_{r,2}\langle N_{fr}\rangle + 2q_{r,3}\langle N_{rr}\rangle)^2} \quad (9)$$

In the following, it is assumed that the corresponding proportionality factors q_f for FAM and q_r for ROX are independent of the different species that can form; i.e., no changes in the quantum yield occur upon protein binding. In this case, it is $q_{r,1} = q_{r,2} = q_{r,3}$ and $q_{f,1} = q_{f,2} = q_{f,3}$ in eq 9 and in eq 11, and the proportionality constants q_f and q_r cancel out. Whether this assumption is justified can be tested by measuring the average fluorescence intensity as given by the count rate of each detection channel in the FCS experiments in the presence and absence of protein. In principle, there are two types of processes that have to be considered which can lead to changes in the quantum yield. The first is nonradiative fluorescence resonance energy transfer (FRET) between two dyes that have a spectral overlap of the emission spectrum of one dye ("donor") and the absorbance spectrum of the other dye ("acceptor") (*26*, *27*). This is the case for the FAM and ROX dyes used here. This donor−acceptor pair has been used for the construction of "energy transfer primers" for DNA sequencing that exhibited the highest energy transfer for a separation distance of about 2−3 nm (reviewed in ref *28*). The efficiency of FRET depends on the sixth power of the separation distance R between the two dyes and decreases rapidly when $R > R_0$. The parameter R_0 is the donor−acceptor separation distance at which 50% transfer occurs. For the FAM−ROX

dye pair, R_0 can be calculated from the overlap integral of the FAM emission spectrum and the ROX absorbance spectrum to be around 5 nm, meaning that transfer with an efficiency of >5% occurs only for separation distances of <8 nm. FRET should lead to a reduced donor fluorescence and an increase in the acceptor fluorescence. It can be detected as described for example in ref *29* and was not observed in the system studied here as judged from fluorescence emission ($\lambda_{ex} = 490$ nm, $\lambda_{em} = 500-750$ nm) and excitation ($\lambda_{ex} = 400-600$ nm, $\lambda_{em} = 610$ nm) spectra (data not shown).

The second process that has to be considered consists of changes in the dye quantum yield due to protein binding. As determined from measurements of the fluorescence intensity, the binding of the unphosphorylated NtrC protein to the ES-2_f or the ES-2_r duplex did not change the quantum yield of both the ROX and the FAM dye. This is consistent with previous fluorescence measurements of NtrC binding to the same DNA sequence but labeled with Texas Red (*25*). Upon phosphorylation of the NtrC protein, a quenching of the relative ROX intensity by about 6% and of the FAM intensity by about 15% was observed when the NtrC-P−DNA complex was formed. This effect has been neglected in the analysis since the resulting error is small compared to the total error of the measurement that includes uncertainties in the determination of the DNA concentration and the NtrC dimer concentration (see above) in addition to errors in the FCCS measurement itself.

For the cross-correlation function with one fluorophore being detected in channel f and the other in channel r, the term $\langle \delta F_f(t)\, \delta F_r(t)\rangle$ in eq 5 is zero, if the detection in the two channels is uncorrelated. This is the case for particles that contain only FAM or only ROX labels. Thus, if we indicate by F' the fluorescence contribution that results solely from particles with both dyes, we can write according to eqs 5 and 6

$$G_x(0) = \frac{\langle \delta F'_f(t)\, \delta F'_r(t)\rangle}{\langle F'_f(t)\rangle\langle F'_r(t)\rangle}\frac{\langle F'_f(t)\rangle\langle F'_r(t)\rangle}{\langle F_f(t)\rangle\langle F_r(t)\rangle} = \frac{1}{\langle N_{fr}\rangle}\frac{\langle F'_f(t)\rangle\langle F'_r(t)\rangle}{\langle F_f(t)\rangle\langle F_r(t)\rangle} \tag{10}$$

In eq 10, the multiplication of eq 5 with the term $[\langle F'_f(t)\rangle\langle F'_r(t)\rangle]/[\langle F'_f(t)\rangle\langle F'_r(t)\rangle]$ allows it to replace the left fraction of eq 10 with $1/\langle N_{fr}\rangle$ according to eq 6. The remaining average fluorescence intensity terms can then be expressed in eq 11 by the average number of particles.

$$G_x(0) = \frac{q_{f,2}q_{r,2}\langle N_{fr}\rangle}{(q_{f,1}\langle N_f\rangle + q_{f,2}\langle N_{fr}\rangle + 2q_{f,3}\langle N_{ff}\rangle)(q_{r,1}\langle N_r\rangle + q_{r,2}\langle N_{fr}\rangle + 2q_{r,3}\langle N_{rr}\rangle)} \tag{11}$$

As discussed above in the context of eq 9, the simplification is introduced that $q_{r,1} = q_{r,2} = q_{r,3}$ and $q_{f,1} = q_{f,2} = q_{f,3}$, and the proportionality constants in eq 11 cancel out. For the analysis of the data in terms of the fraction of complexes that carry two dye molecules, the ratio $G_x(0)/G_{0,r}(0)$ (ratio G) is obtained from eqs 9 and 11:

$$\text{ratio } G = \frac{G_x(0)}{G_{0,r}(0)} = \frac{\langle N_{fr}\rangle(\langle N_r\rangle + \langle N_{fr}\rangle + 2\langle N_{rr}\rangle)}{(\langle N_f\rangle + \langle N_{fr}\rangle + 2\langle N_{ff}\rangle)(\langle N_r\rangle + \langle N_{fr}\rangle + 4\langle N_{rr}\rangle)} \tag{12}$$

In the DNA experiments, particles with two fluorescein or two rhodamine labels were not present and, thus, $\langle N_{ff}\rangle$ and $\langle N_{rr}\rangle$ are 0. In addition, an equimolar ratio of the singly labeled strands was used so that $\langle N_f\rangle = \langle N_r\rangle$. Under these conditions, eq 12 reduces to

$$\text{ratio } G_{DNA} = \frac{G_x(0)}{G_{0,r}(0)} = \frac{\langle N_{fr}\rangle}{\langle N_f\rangle + \langle N_{fr}\rangle} = \frac{\langle N_{fr}\rangle}{\langle N_r\rangle + \langle N_{fr}\rangle} = \theta \tag{13}$$

The parameter θ is the fraction of the total amount of FAM (or ROX) dye label that is present in the doubly labeled duplexes.

In the case of the binding of two DNA duplexes to the octameric protein complex of phosphorylated NtrC, one has to consider also complexes that have two singly labeled DNAs with the same dye. Since the experiments were conducted with the duplexes ES-2_r and ES-2_f that were mixed in a 1:1 ratio, one obtains a binomial distribution of doubly labeled complexes of 1 (two fluorescein labels, N_{ff}) to 1 (two rhodamine labels, N_{rr}) to 2 (one rhodamine and one fluorescein label, N_{fr}). As inferred from gel-shift experiments of NtrC binding to the ES-2_r and ES-2_f duplex, the protein does not discriminate between the two duplexes (data not shown), so the above unbiased distribution is expected. With the total concentration of FAM dye $\langle N_{0,f}\rangle$ and of ROX $\langle N_{0,r}\rangle$, the concentration of the different species can be expressed as shown in eq 14 in terms of the dye fraction θ present in complexes that have two dyes:

$$\begin{aligned} \langle N_{o,f}\rangle &= \langle N_{o,r}\rangle = \langle N_o\rangle \\ \langle N_f\rangle &= \langle N_r\rangle = (1-\theta)\langle N_o\rangle \\ \langle N_{ff}\rangle &= \langle N_{rr}\rangle = \frac{\theta}{4}\langle N_o\rangle \\ \langle N_{fr}\rangle &= \frac{\theta}{2}\langle N_o\rangle \end{aligned} \tag{14}$$

From eqs 6 and 11, we obtain with the definition of θ given above:

$$\text{ratio } G_{NtrC} = \frac{G_x(0)}{G_{0,r}(0)} = \frac{\langle N_{fr}\rangle}{\langle N_f\rangle + 3\langle N_{fr}\rangle} = \frac{\langle N_{fr}\rangle}{\langle N_r\rangle + 3\langle N_{fr}\rangle} = \frac{\theta}{2+\theta} \tag{15}$$

This means for a sample in which all NtrC complexes have two duplexes bound the theoretical value for ratio G_{NtrC} that can be obtained is $^1/_3$ as opposed to the DNA experiments (eq 13) where the theoretical maximum value of ratio G_{DNA} is 1. In practice, these values could not be reached due to incomplete overlap of the excitation focus volumes at the two different excitation wavelengths (488 and 568 nm) and the occurrence of the nonfluorescent triplet state. In addition, even in the case where no molecules with both dyes were

present, a value for $G_x(0)/G_{0,r}(0)$ of >0 was measured, because of cross-talk between the two detection channels. Accordingly, the necessary instrument correction factors were obtained from measurements with a sample containing only the doubly labeled ES-2_{fr} duplex (determination of ratio G_{max}) or only a 1:1 mixture of the singly labeled ES-2_f and ES-2_r duplexes (determination of ratio G_{min}). With these parameters, it follows from eq 15 that the fraction θ of NtrC octamer complexes that have two DNA strands bound is given by

$$\theta = \frac{2(\text{ratio } G_{NtrC} - \text{ratio } G_{min})}{\text{ratio } G_{max} - \text{ratio } G_{NtrC}} \quad (16)$$

The corresponding expression for the DNA experiments according to eq 13 is simply

$$\theta = \frac{\text{ratio } G_{DNA} - \text{ratio } G_{min}}{\text{ratio } G_{max} - \text{ratio } G_{min}} \quad (17)$$

The binding curves obtained for NtrC-P according to the analysis described above were fitted with the program BIOEQS (*30*, *31*) to extract the free energy ΔG for the formation of the different NtrC-P−DNA complexes.

RESULTS

The DNA binding of NtrC-P was studied with the 59 bp ES-2 DNA duplex (*10*, *11*, *25*), the sequence of which is given in Figure 1. ES-2 has two NtrC binding sites and constitutes a DNA enhancer sequence that is sufficient for NtrC to exert its transcriptional activity at low protein concentrations (*10*, *11*). In the experiments, ES-2 duplexes labeled at the 5′-end with 6-carboxyfluorescein (ES-2_f) or 6-carboxy-X-rhodamine (ES-2_r) or with both dyes (ES-2_{fr}) were used (Figure 1).

To demonstrate the validity of the experimental approach and to determine the instrument response factors, the FCS and FCCS measurements were conducted first in the absence of NtrC (Figure 2). In these experiments, the fraction of doubly labeled ES-2_{fr} in a mixture with the singly labeled ES-2_f and ES-2_r was increased, while the total dye concentration was kept constant at 10 nM FAM and 10 nM ROX. Typical cross-correlation curves are shown in Figure 2A. To correct for possible concentration differences between the samples and to derive an expression that is independent of the size of the focus volume, the cross-correlation function $G_x(0)$ was divided by the autocorrelation function $G_{0,r}(0)$ of the rhodamine channel. The ROX dye exhibited a smaller triplet contribution than FAM, and the value of $G_0(0)$ could therefore be determined more accurately. The resulting ratio $G_x(0)/G_{0,r}(0)$ is designated here as ratio *G*. It reflects the relative amount of particles with two different dyes in a manner that is independent of the total fluorophore concentration (*22*). For the DNA experiments, ratio *G* is equivalent to the fraction θ of doubly labeled duplexes (eqs 13 and 17).

The theoretical maximum value for ratio G_{DNA} of 1 could not be reached because the focus volumes for the two different excitation wavelengths (488 and 568 nm) did not completely overlap. This was partly due to the wavelength dependence of the size of the diffraction-limited focal spot and partly due to chromatic aberrations of the optical system. In addition, the occurrence of the nonfluorescent triplet state

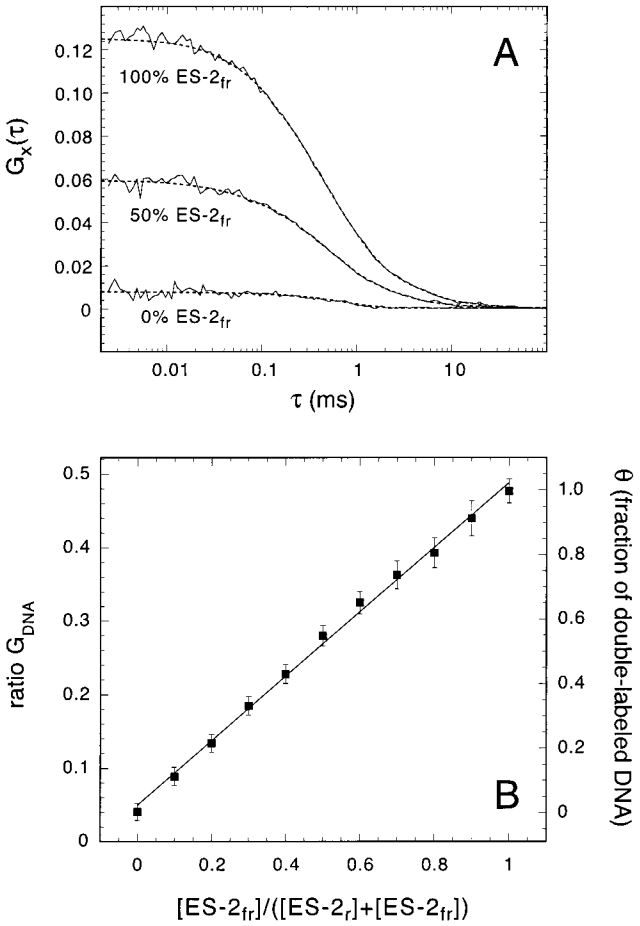

FIGURE 2: FCCS measurements of an increasing fraction of doubly labeled ES-2_{fr} duplexes. The total dye concentration was kept constant at 10 nM fluorescein and 10 nM rhodamine in all experiments. (A) Representative cross-correlation curves: lower curve, 0% ES-2_{fr} (10 nM ES-2_f and 10 nM ES-2_r); middle curve, 50% ES-2_{fr} (5 nM ES-2_f, 5 nM ES-2_r, and 5 nM ES-2_{fr}); and upper curve, 100% ES-2_{fr} (10 nM ES-2_{fr}). The dashed lines show one-component fit curves of the data to eq 7 without a triplet contribution. (B) Plot of the measured ratio *G* vs the fraction of doubly labeled duplex ES-2_{fr}. The concentration of ES-2_f was always identical to that of ES-2_r so that the fraction of ES-2_{fr} is given for each fluorophore by [ES-2_{fr}]/([ES-2_f] + [ES-2_{fr}]) or [ES-2_{fr}]/([ES-2_r] + [ES-2_{fr}]). The fraction θ of doubly labeled DNA (right *y*-axis) was calculated according to eq 17.

also contributes to a reduction of the cross-correlation signal since during the time in which one of the dyes is in the triplet state no cross-correlation signal can be observed. A sample that consisted of only the doubly labeled ES-2_{fr} duplex was therefore used as a reference to determine the experimental maximum, and a value for ratio G_{max} of 0.48 ± 0.02 was obtained (Figure 2B). On the other hand, even in a case where no ES-2_{fr} DNA was present and the sample included only ES-2_f and ES-2_r, a value for ratio *G* of >0 was measured. This was due to cross-talk between the two detection channels and results in an apparent cross-correlation signal that is simply the autocorrelation of singly labeled molecules (*18*, *19*, *21*−*23*). The minimal value for ratio G_{min} determined in the absence of doubly labeled molecules was 0.04 ± 0.01. It was dependent only on the total dye concentration which was the same in all the experiments. With ratio G_{max} and ratio G_{min}, the instrument correction factors were known and the value of θ could be calculated according to eq 17 from the measured ratio G_{DNA}. It is plotted

on the right *y*-axis of Figure 2B. The graph shows the expected linear dependence of θ on the sample composition and demonstrates that a fraction as small as 5% of the doubly labeled molecules could be reliably quantitated. The diffusion times measured for the ES-2_{fr} DNA were 0.32 ± 0.01 ms (FAM autocorrelation), 0.37 ± 0.01 ms (ROX autocorrelation), and 0.42 ± 0.01 ms (cross-correlation). With eq 8, the width of the focus volume w_0 can be calculated from the diffusion times to be 242 ± 38 nm (FAM detection), 260 ± 35 nm (ROX detection), and 279 ± 33 nm (cross-correlation) using the known value for D_{exp} of 4.6×10^{-7} cm^2 s^{-1} for the diffusion constant of the ES-2 DNA under the conditions of the experiment (*10*).

To study whether the octamer complex formed by NtrC-P at the ES-2 enhancer sequence can bind a second DNA duplex, a sample containing a mixture of 10 nM ES-2_f and 10 nM ES-2_r was assessed in the presence of increasing concentrations of NtrC-P under conditions where the protein was phosphorylated (*10*). The results showed an almost linear increase of ratio *G* up to a protein concentration of one NtrC-P dimer per binding site where a value for ratio *G* of 0.148 ± 0.04 was reached (Figure 3). At higher NtrC-P concentrations, a slowly decreasing plateau appeared. This demonstrates that the NtrC-P octamer complex could bind two ES-2 duplexes. In the absence of phosphorylation, no significant increase above the background of 0.04 ± 0.01 was detected (Figure 3B). Thus, only the phosphorylated NtrC-P complex had the ability to bind a second DNA duplex. To exclude the possibility that the observed signal was due to a NtrC-P-catalyzed strand exchange between the singly labeled duplexes, the following experiment was conducted: Complexes of NtrC-P with ES-2 for which the maximum value of ratio *G* had been measured (one NtrC-P dimer per binding site) were incubated with proteinase K. As expected, the value of ratio *G* fell from 0.148 ± 0.04 down to a background signal of 0.06 ± 0.02 upon digestion of the NtrC-P protein. This demonstrates that no strand exchange has taken place and that the observed cross-correlation signal was indeed due to binding of two DNA strands to the NtrC-P octamer.

For the NtrC-P complex with ES-2_f and ES-2_r, a diffusion time τ of 0.90 ± 0.17 ms was determined from a one-component fit of the cross-correlation curves according to eq 7. With the w_0 value of 279 ± 33 nm given above, this corresponds to a diffusion coefficient D_{exp} of $(2.2 \pm 0.5) \times 10^{-7}$ cm^2 s^{-1}. The rotational correlation for this species can be estimated from the Perrin equation to be about 200 ns with the data given in ref *10* (molecular mass of 507 kDa, a partial specific volume of 0.711 mL/g, and a buffer viscosity of 1.182 mPa s). This is a factor of 10 smaller than the shortest correlation times of 2 μs used in the analysis of the data and several orders of magnitude below the translational diffusion time τ of 0.90 ± 0.17 ms. Thus, although the laser excitation was with linearly polarized light, any polarization effects on the detected fluorescence signal can be neglected because during the time of the measurement all orientations of the complex are sampled and averaged.

From the measured ratio *G*, the fraction θ of DNA found in NtrC-P complexes with two DNA strands was calculated according to eq 16 (Figure 3B). At a NtrC concentration of one dimer per binding site, a maximum θ value of 0.7 was measured; i.e., under these conditions, 70% of the DNA was

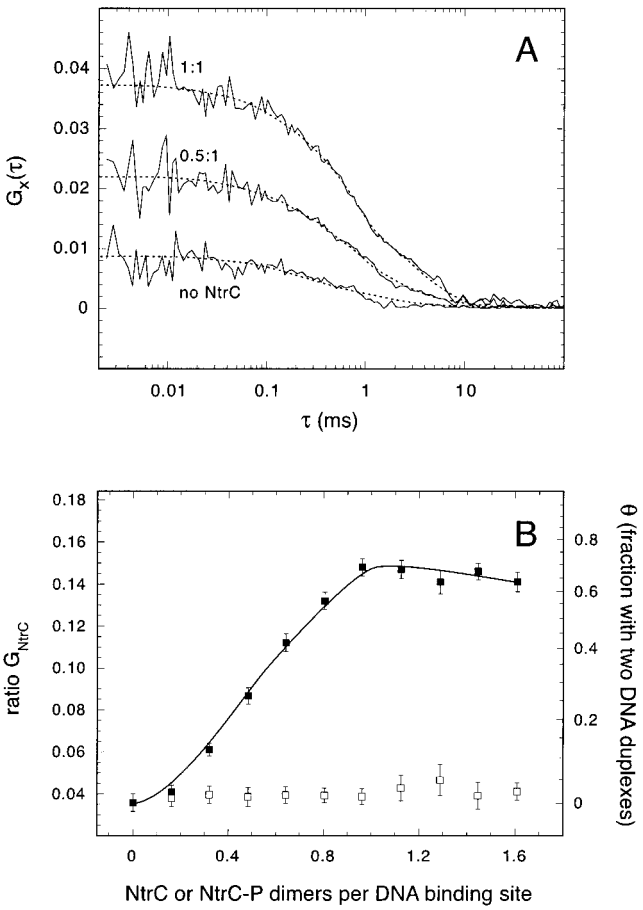

FIGURE 3: FCCS measurements of NtrC and NtrC-P binding to the ES-2 DNA duplex. Samples containing a mixture of 10 nM ES-2_f and 10 nM ES-2_r (equivalent to a total of 20 nM duplexes or 40 nM NtrC binding sites) were incubated with the indicated NtrC protein concentrations as described in Materials and Methods. (A) Representative cross-correlation curves: lower curve, no NtrC added; middle curve, 0.5 NtrC-P dimer per binding site; and upper curve, one NtrC-P dimer per binding site. The dashed lines show one-component fit curves to eq 7 without a triplet contribution. (B) The measured ratio *G* is plotted vs the protein concentration given in NtrC or NtrC-P dimers per binding site. Experiments were conducted with phosphorylated NtrC-P (■) and with unphosphorylated protein (□). The fraction θ of DNA in complexes with two strands is shown on the right *y*-axis (note that the scale is not linear). As described in the text, θ was derived from ratio *G* according to eq 16. The solid lines for NtrC-P represent the fit curve determined according to the model described in eq 18 in which three complexes can form: a DNA duplex with two NtrC-P dimers (DN_2), a DNA duplex with four NtrC-P dimers (DN_4), or a complex with four NtrC-P dimers and two DNA strands (D_2N_4).

present in NtrC-P complexes with two ES-2 molecules. The NtrC-P binding curves were acquired under conditions where the frequently used simplification that the concentration of free protein is approximately equal to the total protein concentration was not valid. In this case, analytical expressions for multiple binding equilibria are very complex. Therefore, a numerical analysis of the data was conducted with the program BIOEQS (*30*, *31*). BIOEQS fits the ΔG of formation of each species for a given model to the experimental data. The simplest model that resulted in a good fit of the data presented in Figure 3 was obtained with three different NtrC−DNA complexes as shown in eq 18. In these reaction schemes, D represents one ES-2 DNA and N one NtrC-P dimer. From the fit, the following ΔG values for the

formation of each species were derived:

$$D + 2N \rightleftarrows DN_2 \qquad \Delta G_1 = 26.3 \pm 1.3 \text{ kcal/mol}$$
$$D + 4N \rightleftarrows DN_4 \qquad \Delta G_2 = 46.2 \pm 4.0 \text{ kcal/mol} \qquad (18)$$
$$2D + 4N \rightleftarrows D_2N_4 \qquad \Delta G_3 = 63.6 \pm 2.7 \text{ kcal/mol}$$

The analysis of the FCCS data revealed that at the lowest protein concentrations only the D_2N_4 and the DN_2 complex were formed. Once all NtrC binding sites were occupied, any further increase in the protein concentration led to the conversion of D_2N_4 and DN_2 into the DN_4 complex, which consists of four NtrC-P dimers and one ES-2 duplex.

DISCUSSION

Previously, a value for ΔG of 23.2 ± 1.8 kcal/mol in the absence of ATP was measured by fluorescence anisotropy for the noncooperative binding of two unphosphorylated NtrC dimers to the same DNA under similar conditions (*25*). It is known that phosphorylation leads to a strong cooperativity of NtrC-P binding (*1*, *2*, *11*, *32*, *33*). The ΔG value of 26.3 ± 1.3 kcal/mol determined here for the binding of two NtrC-P dimers (formation of the DN_2 complex in eq 18), as well as the ΔG values for the octamer complexes DN_4 and D_2N_4, is consistent with previous measurements (*11*, *32*, *33*). The free energy difference is about 3 kcal/mol for the DN_2 species as compared to the binding of two unphosphorylated protein dimers in the absence of ATP. Thus, the quantitative analysis of the FCCS data in terms of the stability of the different NtrC-P−DNA species yields values that are compatible with the data determined by other techniques. Furthermore, the results of the FCCS experiments demonstrate clearly that the octamer complex of NtrC-P can simultaneously bind two DNA duplexes as shown in the scheme depicted schematically in Figure 4A. Such an interaction has been proposed to explain the results from molecular weight determinations by analytical ultracentrifugation at various NtrC/DNA ratios (*10*). On the basis of these experiments, hydrodynamic models for the different NtrC− and NtrC-P−DNA complexes were constructed. For the model of the NtrC-P octamer with two ES-2 duplexes (Figure 4A), a diffusion constant D_{exp} of 1.9×10^{-7} cm^2 s^{-1} has been calculated (*10*). This is very similar to the D_{exp} value of $(2.2 \pm 0.5) \times 10^{-7}$ cm^2 s^{-1} determined here from the measured diffusion time of 0.90 ± 0.17 ms in the FCCS curves. According to the hydrodynamic model, the two dyes would have a separation distance of 20−30 nm (Figure 4A). In agreement with this conformation, no energy transfer between FAM and ROX was measured since this separation distance is well above the detection limit of ≈8 nm for the FAM−ROX dye pair as explained in Materials and Methods.

In previous electron microscopy and scanning force microscopy studies, wrapping of the DNA around multimers of a constitutively active NtrC mutant has been observed (*7*, *34*), as well as tethering of two enhancer-containing DNA fragments by NtrC-P for some of the molecules that were studied (*15*). However, these experiments do not provide direct evidence for the presence of two independent DNA binding sites at the NtrC-P enhancer complex. As demonstrated for *Escherichia coli* RecA protein, simultaneous binding of two DNA strands can also be identified with an accurate measurement of the binding stoichiometry of DNA to protein monomer (*35*). In the case of NtrC, this approach is not applicable, since a stoichiometry of two NtrC-P dimers per DNA strand would not be indicative for the formation of a complex in which two DNA strands are bound. Thus, the two-color fluorescence cross-correlation experiments presented here provide a new approach that offers unique possibilities since the presence of multiple ligands of a protein complex can be directly revealed. In addition, the experiments were conducted in buffer solution under physiological salt and protein concentrations and at equilibrium. As shown for the analysis of *Eco*RI activity, kinetic FCCS experiments are also possible with the current time resolution limit being around 1 s (*20*, *21*). Such experiments should also provide interesting information about the kinetics of DNA binding and multimerization of NtrC-P.

The method described here for the analysis of the FCS/FCCS data allows a quantitative evaluation of the binding curves. Under optimal conditions, the majority of the DNA (about 70%) was found to be present in NtrC-P complexes

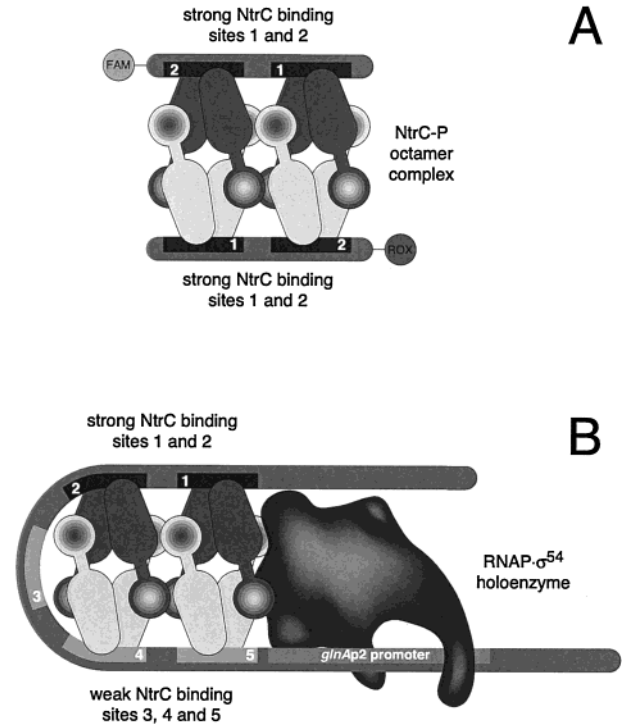

FIGURE 4: Schematic models for the NtrC-P complex with DNA. (A) The octameric complex of NtrC-P with one ES-2_f and one ES-2_r duplex as detected in the FCS/FCCS measurements is shown. Two NtrC dimers drawn in dark or light gray are bound directly to one duplex. Upon phosphorylation of the NtrC receiver domain (represented by a gray-scale gradient), they can associate with each other to form an octamer complex with two separate DNA strands. In the scheme, the two dyes are located on opposite sides of the complex (antiparallel orientation). Since the NtrC binding sites are symmetric, a parallel orientation is equally possible. For a hydrodynamic model of the NtrC-P complex with the ES-2 DNA, see ref *10*. According to this model, the separation distance between the two dyes is about 30 nm for an antiparallel orientation and 20 nm for a parallel orientation. (B) Schematic model for a possible conformation of the looped intermediate formed between the octamer complex of NtrC-P and RNAP·σ^{54} at the *glnA*p2 promoter. Two NtrC dimers are bound to strong sites 1 and 2 (template positions −148 to −132 and −116 to −100). Two additional NtrC dimers (light gray) can associate with the two DNA-bound dimers to form a NtrC octamer complex and could interact with the weak binding sites close to the promoter.

with two DNA strands. Thus, the existence of two independent DNA binding sites appears to be a general feature of the NtrC-P enhancer complex. This result could have important implications for the conformation of the looped intermediate between NtrC-P and RNAP•σ^{54}, since the NtrC-P complex at the enhancer could bind to the DNA at an additional site while contacting the polymerase. Such an interaction would be facilitated by NtrC binding sites close to the promoter sequence. Interestingly, three weak binding sites are found upstream of the *glnA*p2 promoter at positions −94 to −81, −73 to −60, and −53 to −37 in addition to the two strong binding sites at positions −148 to −132 and −116 to −100. The latter two sites are essential and sufficient for the activation reaction (*1*, *2*). However, if the three weak binding sites were replaced with a random DNA sequence, the kinetic rate of open complex formation was 3 times slower than with the wild-type DNA sequence as determined in vitro with superhelical templates (A. Schulz, J. Langowski, K. Rippe, manuscript in preparation). A corresponding reduction in the extent of open complex formation under equilibrium conditions has been reported previously (*36*, *37*). However, the results have been attributed to the presence of an intrinsically curved DNA sequence between enhancer and promoter in the wild-type sequence. In light of the results described here, the weak NtrC binding sites found upstream of the *glnA*p2 promoter could also facilitate the formation of the looped intermediate with RNAP•σ^{54} by simultaneous interactions of the NtrC-P octamer complex with the two strong and one or more of the three weak binding sites. This is shown schematically in Figure 4B. Such a conformation would also explain the observed wrapping of DNA around NtrC multimers as well as binding to "spiral" DNA inserts lacking specific NtrC sites (*7*, *34*, *38*). Binding of NtrC to the three weak sites has been observed in vitro at relatively high protein concentrations (*39*, *40*). With in vivo footprinting experiments, a protection of the DNA was detected only for strong NtrC sites 1 and 2 (*41*). The degree of protection observed in this type of experiment reflects the occupancy of the sites that are being studied. Therefore, it is unlikely that NtrC-P binding to the weak sites during formation of the loop complex would be observed, since the contact of the NtrC-P enhancer complex with RNAP•σ^{54} at the promoter appears to be transient (*12*). This feature of the system makes it difficult to study the conformation of the looped intermediate. With techniques such as FCS/FCCS, the detection and analysis of single molecules in solution is possible and new approaches to addressing this problem become available.

ACKNOWLEDGMENT

I am grateful to Jörg Langowski, Michael Tewes, Malte Wachsmuth, and Thomas Weidemann for valuable discussions and help with the fluorescence correlation spectroscopy experiments and to Alexandra Schulz for a preparation of NtrC protein and critical reading of the manuscript. In addition, I thank one of the reviewers of the paper for constructive criticism.

REFERENCES

1. Magasanik, B. (1996) in *Escherichia coli and Salmonella* (Neidhardt, F. C., Ed.) pp 1344−1356, ASM Press, Washington, DC.
2. Porter, S. C., North, A. K., and Kustu, S. (1995) in *Two-Component Signal Transduction* (Hoch, J. A., and Silhavy, T. J., Eds.) pp 147−158, ASM Press, Washington, DC.
3. Reitzer, L. J., Movsas, B., and Magasanik, B. (1989) *J. Bacteriol. 171*, 5512−5522.
4. Su, W., Porter, S., Kustu, S., and Echols, H. (1990) *Proc. Natl. Acad. Sci. U.S.A. 87*, 5504−5508.
5. Wedel, A., Weiss, D. S., Popham, D., Dröge, P., and Kustu, S. (1990) *Science 248*, 486−490.
6. Gralla, J. D., and Collado-Vides, J. (1996) in *Escherichia coli and Salmonella* (Neidhardt, F. C., Ed.) pp 1232−1245, ASM Press, Washington, DC.
7. Rippe, K., Guthold, M., von Hippel, P. H., and Bustamante, C. (1997) *J. Mol. Biol. 270*, 125−138.
8. Feng, J., Atkinson, M. R., McCleary, W., Stock, J. B., Wanner, B. L., and Ninfa, A. J. (1992) *J. Bacteriol. 174*, 6061−6070.
9. Reitzer, L. J., and Magasanik, B. (1983) *Proc. Natl. Acad. Sci. U.S.A. 80*, 5554−5558.
10. Rippe, K., Mücke, N., and Schulz, A. (1998) *J. Mol. Biol. 278*, 915−933.
11. Porter, S. C., North, A. K., Wedel, A. B., and Kustu, S. (1993) *Genes Dev. 7*, 2258−2273.
12. Rombel, I., North, A., Hwang, I., Wyman, C., and Kustu, S. (1998) *Cold Spring Harbor Symp. Quant. Biol. 63*, 157−166.
13. Austin, S., and Dixon, R. (1992) *EMBO J. 11*, 2219−2228.
14. Mettke, I., Fiedler, U., and Weiss, V. (1995) *J. Bacteriol. 177*, 5056−5061.
15. Wyman, C., Rombel, I., North, A. K., Bustamante, C., and Kustu, S. (1997) *Science 275*, 1658−1661.
16. Eigen, M., and Rigler, R. (1994) *Proc. Natl. Acad. Sci. U.S.A. 91*, 5740−5747.
17. Maiti, S., Haupts, U., and Webb, W. W. (1997) *Proc. Natl. Acad. Sci. U.S.A. 94*, 11753−11757.
18. Schwille, P., Meyer-Almes, F. J., and Rigler, R. (1997) *Biophys. J. 72*, 1878−1886.
19. Rigler, R., Foldes-Papp, Z., Meyer-Almes, F. J., Sammet, C., Volcker, M., and Schnetz, A. (1998) *J. Biotechnol. 63*, 97−109.
20. Kettling, U., Koltermann, A., Schwille, P., and Eigen, M. (1998) *Proc. Natl. Acad. Sci. U.S.A. 95*, 1416−1420.
21. Koltermann, A., Kettling, U., Bieschke, J., Winkler, T., and Eigen, M. (1998) *Proc. Natl. Acad. Sci. U.S.A. 95*, 1421−1426.
22. Tewes, M. (1998) Ph.D. Thesis, Ruprecht-Karls-Universität Heidelberg, Heidelberg, Germany.
23. Langowski, J., and Tewes, M. (2000) in *Protein-DNA Interactions: A Practical Approach* (Buckle, M., and Travers, A., Eds.) Oxford University Press, Oxford, U.K.
24. Palmer, A. G., and Thompson, N. L. (1987) *Biophys. J. 52*, 257−270.
25. Sevenich, F. W., Langowski, J., Weiss, V., and Rippe, K. (1998) *Nucleic Acids Res. 26*, 1373−1381.
26. Förster, T. (1948) *Ann. Phys. 2*, 55−75.
27. Förster, T. (1951) *Fluoreszenz organischer Verbindungen*, Vandenhoeck & Ruprecht, Göttingen, Germany.
28. Glazer, A. N., and Mathies, R. A. (1997) *Curr. Opin. Biotechnol. 8*, 94−102.
29. Clegg, R. M. (1992) *Methods Enzymol. 211*, 353−388.
30. Royer, C. A., and Beechem, J. M. (1992) *Methods Enzymol. 210*, 481−505.
31. Royer, C. A. (1993) *Anal. Biochem. 210*, 91−97.
32. Chen, P., and Reitzer, L. J. (1995) *J. Bacteriol. 177*, 2490−2496.
33. Weiss, V., Claverie-Martin, F., and Magasanik, B. (1992) *Proc. Natl. Acad. Sci. U.S.A. 89*, 5088−5092.
34. Révet, B., Brahms, S., and Brahms, G. (1995) *Proc. Natl. Acad. Sci. U.S.A. 92*, 7535−7539.
35. Zaitsev, E. N., and Kowalczykowski, S. C. (1999) *J. Mol. Biol. 287*, 21−31.
36. Carmona, M., and Magasanik, B. (1996) *J. Mol. Biol. 261*, 348−356.
37. Carmona, M., Claverie-Martin, F., and Magasanik, B. (1997)

Proc. Natl. Acad. Sci. U.S.A. 94, 9568−9572.

38. Brahms, G., Brahms, S., and Magasanik, B. (1995) *J. Mol. Biol. 246*, 35−42.
39. Hirschman, J., Wong, P. K., Sei, K., Keener, J., and Kustu, S. (1985) *Proc. Natl. Acad. Sci. U.S.A. 82*, 7525−7529.
40. Ninfa, A. J., Reitzer, L. J., and Magasanik, B. (1987) *Cell 50*, 1039−1046.
41. Sasse-Dwight, S., and Gralla, J. D. (1988) *Proc. Natl. Acad. Sci. U.S.A. 85*, 8934−8938.

BI9922190